Yttrium oxide thin films: Influence of the oxygen vacancy network organization on the microstructure

Michaël Jublot, Fabien Paumier, Frédéric Pailloux, Bertrand Lacroix, E. Leau, Philippe Guérin, Marc Marteau, Dominique Imhoff, Michel Jaouen, Rolly Jacques Gaboriaud

Yttrium oxide thin films: Influence of the oxygen vacancy network organization on the microstructure

M. Jublot [a], F. Paumier [a], F. Pailloux [a], B. Lacroix [a], E. Leau [a], P. Guérin [a], M. Marteau [a], M. Jaouen [a], R.J. Gaboriaud [a,*], D. Imhoff [b]

[a] *Laboratoire de Métallurgie Physique, Université de Poitiers, CNRS-SP2MI-BP 30179-86962, Chasseneuil-Futroscope Cedex, France*
[b] *Laboratoire de Physique des Solides, CNRS/Université Paris-Sud, UMR 8502, 91405 Orsay, France*
[*] Corresponding author: rolly.gaboriaud@univ-poitiers.fr (R.J. Gaboriaud).

Abstract

Y_2O_3 thin films are deposited by ion beam sputtering on Si, $SrTiO_3$ and MgO substrates. In order to obtain a better knowledge on the phase transition mechanisms in yttrium oxide, the effects of ion implantation have been studied as a function of the initial microstructure of thin films. The different microstructures for the as-deposited and implanted samples have been studied and characterized by means of X ray diffraction, *High Resolution Transmission Electron Microscopy* and *Electron Energy Loss Spectroscopy* and are compared to the cubic-C and monoclinic-B phase of Y_2O_3. The experimental results show clearly the presence of non-equilibrium phases in the implanted and non-implanted thin films. A particular attention is paid to the understanding of the relationship between the oxygen vacancy network organization, the stoichiometry and the formation mechanisms of these crystallographic phases.

Keywords: Rare Earth Oxyde; Thin film; Crystallographic phases; Oxygen vacancy network

Introduction

It has been shown in a previous work that the micro and nanostructure of the thin film oxide together with the interface composition play a major role in the expected dielectric prop- erties. It is therefore of prime interest to point out what are the crystallographic phases present in the oxide and what might be the consequence of the occurrence of new phases on the physical properties. It is for these reasons that this work is devoted to the different crystallographic phase obtained in the as-deposited sample and after annealing treatments or artifi- cially after ion implantation. Y_2O_3 has attracted much attention because of several phys- ical properties (high *k*: 10-18), wide band gap (5.5 eV) par- ticularly relevant for MOS devices. Y_2O_3 thin films are deposited by ion beam sputtering on Si, $SrTiO_3$ and MgO substrates. Whatever the deposition techniques are, the thin films show a particular structure at the nanometer scale and/or at the oxide/substrate interface. The different microstructures of the as-deposited and implanted samples have been studied and characterized by means of X ray diffraction, High Resolution Transmission Electron Microscopy (HRTEM) and Electron Energy Loss Spectroscopy (EELS) and are compared to the cubic-C (Ia3) Y_2O_3 phases. The experimental results clearly show the presence of non-equilibrium phases in the implanted and non-implanted thin films. The oxygen vacancy network organization seems to be of prime importance in the formation mechanisms of these crystallographic phases.

1. Experiments

Yttrium oxide thin films were deposited by ion beam sput- tering (IBS). The IBS experiments are performed in a Nordiko sputtering apparatus chamber at 700 °C [1]. An RF ion source delivers a 1.2 keV argon beam with an intensity of 80 mA, which sputters a water-cooled 10 cm diameter Y_2O_3 target. The 2.6×10^{-6} Pa background pressure increases to 1.3×10^{-2} Pa during the deposition process. The oxygen partial pressure estimated from the oxygen flow introduced in the sputtering chamber was 4.10^{-3} Pa. The thin films of oxide where deposit- ed on (001)-Si, MgO and $SrTiO_3$ single crystalline substrates [2]. The as-deposited sample of Y_2O_3 have been irradiated by both medium (220 keV Xe^{2+}) and high energy (92 MeV Xe^{23+}) xenon ions by means of a 200 kV ion implantor and by using the irradiation facilities of the GANIL accelerator (Grand Accélérateur National d'Ions Lourds) in Caen respectively. The post annealing treatments

of the as-deposited thin films were per- formed in a quartz tube furnace in air or under a vacuum of roughly 1×10^{-6} Pa at 700 °C. The X-ray diffraction study of the thin films has been performed with a 4-circle Siefert goniometer using the CuKα radiation (0.15406 nm). The X-ray data show that the as-deposited thin films of Y_2O_3 are under a strong compressive stress of 5 GPa which is relaxed by a post- annealing treatments [2]. HRTEM investigations have been performed with a JEOL 3010 high-resolution electron micros- copy (Cs= 1.2 mm) operated at 300 kV (0.19 nm point resolution). The energy-loss near-edge structure (ELNES) spectra have been acquired with a dedicated VG-HB501 scanning transmission electron microscopy (STEM) operated at 100 kV and equipped with a GATAN-PEELS spectrometer (0.2 eV energy dispersion, about 0.7 eV energy resolution and 1 nm spatial resolution).

2. Results and discussion

Ion beam sputtering deposition of the thin films of Y_2O_3 promotes a very particular crystallographic structure whatever the substrates are. As shown in Fig. 1 the samples exhibit a Bragg peak which is non-symmetric with a vertex rather far from the equilibrium angle value of the well-known cubic-C structure of Y_2O_3 (a_0 = 1.0604 nm). On Si and MgO substrates, the out-of-plane reflection is due to the (222) planes. On $SrTiO_3$ the out-of-plane reflection is due to the (400) planes. The thin oxide films grow with a texture on Si and epitaxially on MgO and $SrTiO_3$ with respectively four variants and one variant. The compressive stress of 5 GPa which is obtained from X-ray experiments is due to the so-called penning effect [3] coming from the argon ions of the primary sputtering beam back- scattered on the Y_2O_3 target which knock the sample as the growth of the thin film proceeds. The result is the coexistence of three crystallographic phases: the cubic fluorite-like (Fm3m) structure, the cubic-C (Ia3) structure and a monoclinic structure. These different phases lead to the interpretation of the X-ray non-symmetric Bragg peak by the convolution of three Bragg peaks corresponding to the three different phases as described in Fig. 1. By others deposition techniques as electron beam evaporation [4] or RF-Magnetron sputtering [5], the Y_2O_3 thin films exhibit only one crystallographic phase: the cubic-C. In both cases, the growth direction is Y_2O_3(222) plane parallel to the Si(100) plane.

After annealing at 700 °C for 2 h in air or under vacuum a change in the crystallographic structures of the Y_2O_3 as- deposited thin film appears which gives only one structure which is the cubic-C structure. These observations are explained in a previous investigation [6]. The electrical measurements on Y_2O_3 thin films deposited on Si substrate show a strong shift of the C-V curves according to the annealing under vacuum or under an air atmosphere at 700 °C. TEM investigations showed respectively two thin layers of an yttrium silicate and SiO_x after annealing under vacuum and just one SiO_x layer after annealing under air [7]. Obviously the composition of the interface as well as the crystallographic phase of the Y_2O_3 thin film which is closed to the interface turns out to be of prime importance in the expected electronic property which is necessary for a device engineering.

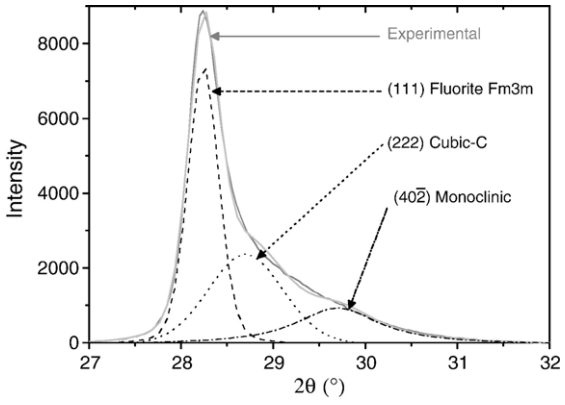

Fig. 1. (2 2 2) in-plane Bragg peak of the as-deposited Y_2O_3 thin film on MgO. Explanation of the non-symmetric shape of the diffraction peak.

2.1. Interfacial phases in epitaxial Y_2O_3 grown on MgO

Y_2O_3 thin films deposited on (001)-MgO substrates have been investigated by HRTEM and EELS spectroscopy. These two techniques have been coupled with an image processing and ab-initio self-consistent full multiple scattering (SC-FMS) calculations, which constitute a powerful set of investigation methods for structural and chemical analysis of

interfaces. The EELS investigation has been focused on the *ELNES* profile of the O K-edge.

Fig. 2 shows an HRTEM image of the Y_2O_3/MgO interface seen along a b110N-MgO direction. The interface between the thin film and the substrate is well defined and quite sharp. The Fig. 2(d) corresponds to the power spectrum (PS) of the image of Fig. 2(a). The brightest spots observed in this PS are related to the cubic-C phase of Y_2O_3, which constitutes the main part of the thin film. The additional spots present in the PS arise from minority grains nucleated on the MgO surface during the first stages of the growth, as shown by the phase-shift reconstruction method. Fig. 2(b)(c) and (d), respectively, show the amplitude of the inverse Fourier transform (IFT) and the phase-shift image after a Bragg filtering around the extra-spot marked by a circle on the PS. These pictures clearly show the presence of grains in which the crystallographic structure is different from that of the rest of the film (Ia3). The positions of the spots related to these grains are in good agreement with those of a monoclinic-B structure (C2/m) of the yttrium oxide seen along the [$1\bar{3}2\bar{}$] direction [8,9]. The extra-spots A and B used to show the amplitude of IFT correspond respectively to the plans (111) and (310).

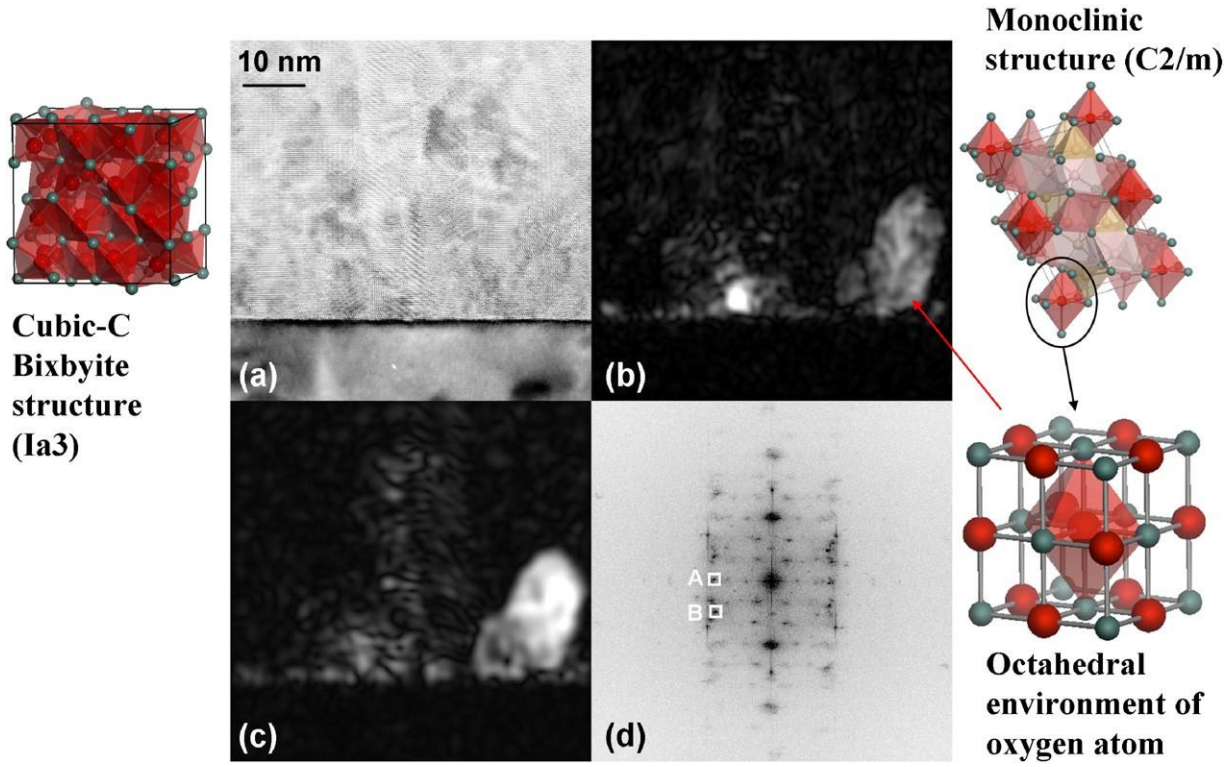

Fig. 2. (a) HRTEM image of the Y_2O_3 /MgO interface. (b) Amplitude of the IFT after filtering with spot A. (c) Amplitude of the IFT after filtering with spot B. (d) IFT amplitude of the HRTEM image.

In order to obtain additional insights about these grains, EELS experiments have been carried out and described in detail elsewhere [10]. Three characteristic profiles of the O K-edge are depicted in Fig. 3(a). One corresponds to the O K-edge in the MgO substrate (spectrum A). The two others are related to different locations of the probe on the yttrium oxide film. The same analysis performed in a region far from the interface, in the yttrium oxide film, reveals only one crystallographic phase corresponding to the spectrum B. By the use of SC-FMS calculations, positions and intensity of the peaks are quite well reproduced with a cluster of only 33 atoms corresponding to the Ia3 phase of Y_2O_3. This confirms the observations from HRTEM. The third shape of O K-edge (spectrum C) is obtained in the Y_2O_3 thin film near the interface with MgO. By comparison with the spectrum (B), it exhibits a third peak c′ and a reversal of the intensity of the two first peaks a′ and b′. This last kind of spectrum (C) is assigned to the grains revealed by the phase-shift reconstruction. We have performed SC-FMS calculations for the monoclinic C2/m structure which was sug- gested by the analysis of the HRTEM images. The calculations have to be performed for the five different Wyckoff positions of the oxygen and the results have to be summed. The resulting spectrum does not match at all with the experiment (not shown here). But the calculation performed for the site 2b seems to be close to the experimental spectrum C. In this site the oxygen atom is surrounded by an octahedral cage of yttrium atoms. Therefore the calculations started with a regular octahedron, which was subsequently distorted to reach a good match between the experiment and the theory. The spectrum which is in good agreement with the experiment spectrum is shown in Fig. 3(b). From this observation, it seems

that off-stoichiometric grains of yttrium oxide are nucleated at the surface of substrate. Indeed, the structure which has been used for this calculations is close to YO rather than $YO_{1.5}$. Obviously, it seems that these grains crystallize in a non-cubic structure in which the main atomic unit might be an octahedron composed of one oxygen atom surrounded by six yttrium atoms.

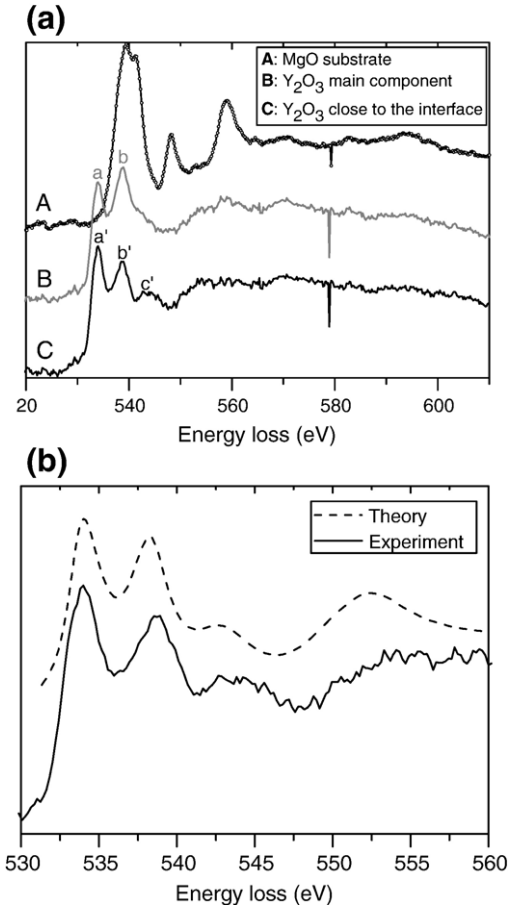

Fig. 3. (a) Main components of the O K-edges in the vicinity of the film/ substrate interface. (b) Comparison between the O K-edge in interfacial grains and SC-FMS calculations performed for an octahedral environment.

2.2. Radiation-induced phase transformations in Y_2O_3 thin films

The as-deposited Y_2O_3 thin films and annealing Y_2O_3 thin films are implanted with 220 keV Xe^{2+} ions at normal incidence. These films have a thickness of 100 nm. Ion fluence is 3.6×10^{19} Xe^{2+}/m^2. The irradiations were performed at liquid nitrogen temperature using a constant ion flux of 1.3×10^{16} Xe^{2+}/m^2 s. Ion flux was kept low in order to minimize sample heating effects. The Monte Carlo program SRIM2003 [11] was used to estimate the ion range profile, the damage energy and the displacement damage distribution in the thin film. Fig. 4 shows the result of this simulation. The peak in the displaced atom damage distribution occurs at a sample depth of 35 nm (corresponding to a peak displacement damage level of 22 displacements per atom (dpa) at fluence 3.63×10^{19} Xe^{2+}/m^2), while the Xe ion range profile reaches a maximum at a depth of 56 nm (corresponding to a peak implantation concentration of 0.9 at.% Xe).

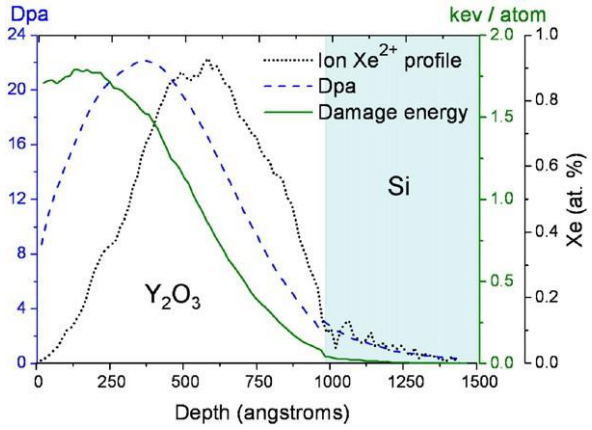

Fig. 4. Monte Carlo simulation results showing the displacement damage profile and the damage energy profile as a function of depth and the ion depth distribution for 220 keV Xe^{2+} ion irradiation of 100 nm Y_2O_3 thin film with a fluence of 3.6×10^{19} Xe^{2+}/m^2. The threshold for atomic displacements for both Y and O were taken to be respectively 25 eV and 28 eV in the calculations.

Fig. 5 shows the results obtained from XRD characterization of as-deposited (b) and annealing (a) Y_2O_3 thin films on silicon substrate before and after Xe^{2+} ion irradiation. In Fig. 5(a) no structural modification is observed between the non-implanted $((222)^{cubic\text{-}C}$ Bragg peak at $2\theta = 29.1°$) and the implanted sample $((222)^{cubic\text{-}C}$ Bragg peak at $2\theta = 29.2°$). In Fig. 5(b) the Bragg peaks correspond to the in-plane reflection. XRD clearly reveals a change in the crystallographic structure of Y_2O_3. The peak corresponding to the fluorite and cubic-C phase at respectively 28.2° and 29.1° shown in Fig. 1 has almost disappeared. Furthermore new peaks emerge in the diffraction pattern. A strong peak appears at 30.5° with a shoulder on the left. A rather small peak is observed around 29°. The peak observed at 30.5° corresponds to the (40-2) reflections and the shoulder ($2\theta = 29.85°$) corresponds to the (401) reflections of the monoclinic phase of Y_2O_3. The transformation from a cubic-C to a monoclinic-B structure has been observed previously in an irradiated sesquioxide [12] where a transformation from cubic-C structured Dy_2O_3 to monoclinic-B Dy_2O_3 is brought about by a 300 keV Xe ions irradiation.

By comparison with the diffractogram obtained before implantation, it is shown that the fluorite phase present in the as-deposited sample completely disappears and become a mono- clinic phase. Nevertheless, a small amount of cubic-C phase is still observed. This phase transformation which is obtained in Y_2O_3 thin film on Si substrate is also observed in the same condition of implantation and thickness with MgO and $SrTiO_3$ susbstrates. When the substrate is $SrTiO_3$ the Y_2O_3 thin film grows in the [400] direction with a unique variant. Therefore the Bragg peak of the {400} planes from the cubic-C and of the (200) planes from the fluorine present in the as-deposited sample disappear and become in majority the (003) planes from the monoclinic phase.

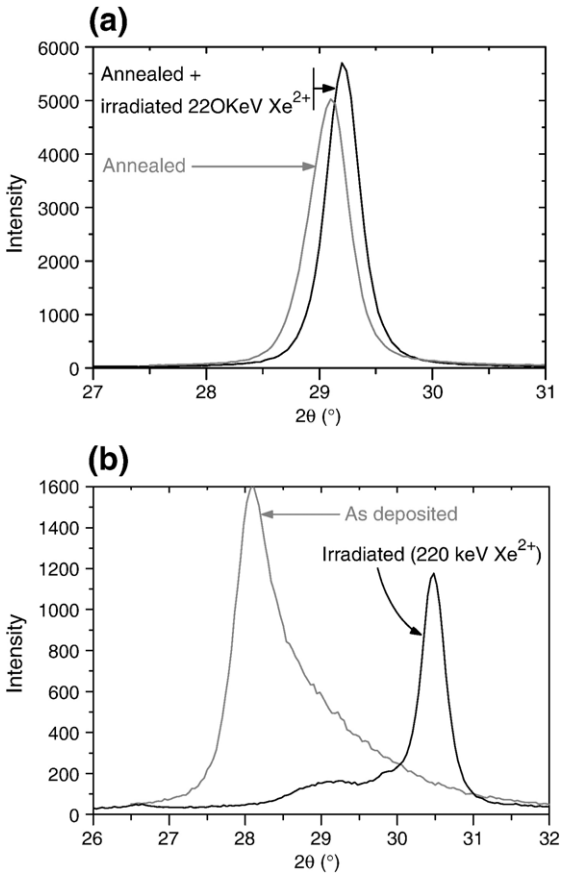

Fig. 5. XRD diffractometer scans obtained from unirradiated and irradiated Y_2O_3 thin film annealed (a) and as-deposited (b). The irradiation was performed with 220 keV Xe^{2+} ions with a fluence of 3.6×10^{19} Xe^{2+}/m^2. The thickness of the thin film of Y_2O_3 deposited silicon is 100 nm.

This transformation is not complete as observed in the HRTEM image of Fig. 6. Fig. 6 shows a picture of Y_2O_3 thin film cross section on $SrTiO_3$ irradiated by 220 keV Xe^{2+} ions with a fluence of 3.63×10^{19} Xe^{2+}/m^2. On the right side are the digital diffractograms of different zones of the HR image. It is shown that the Y_2O_3 thin film is divided into three zones. Near the surface and near the interface with $SrTiO_3$, the digital diffractograms are characteristic of a [100]-Y_2O_3 cubic diffraction pattern (Fig. 6(a)). But in the middle part of the thin film, the digital diffractogram is different compared with the top and the bottom part of the film. The digital diffractogram shown in Fig. 6(b) corresponds to [010]-Y_2O_3 monoclinic diffraction pattern. From the X-ray, pole figure obtained for particular values of 2θ which are characteristic of the monoclinic phase, 24 epitaxial variants of the monoclinic phase are observed. Therefore, from the unique cubic variant of the as-deposited sample, the irradiation induces a coherent phase change in 24 epitaxial variants of a monoclinic phase. From these observations the relationships between the different orientations between the monoclinic and the cubic crystal can be obtained. The $\{222\}^C$ planes correspond to the $(40\text{-}2)^B$, $(310)^B$, $(\text{-}112)^B$, $(401)^B$, $(003)^B$. The $\{400\}^C$ planes correspond to the planes $(310)^B$, $(\text{-}112)^B$, $(401)^B$, $(003)^B$. All these relationships have been observed by diffraction pattern studies. These results are conformed by EELS investigation.

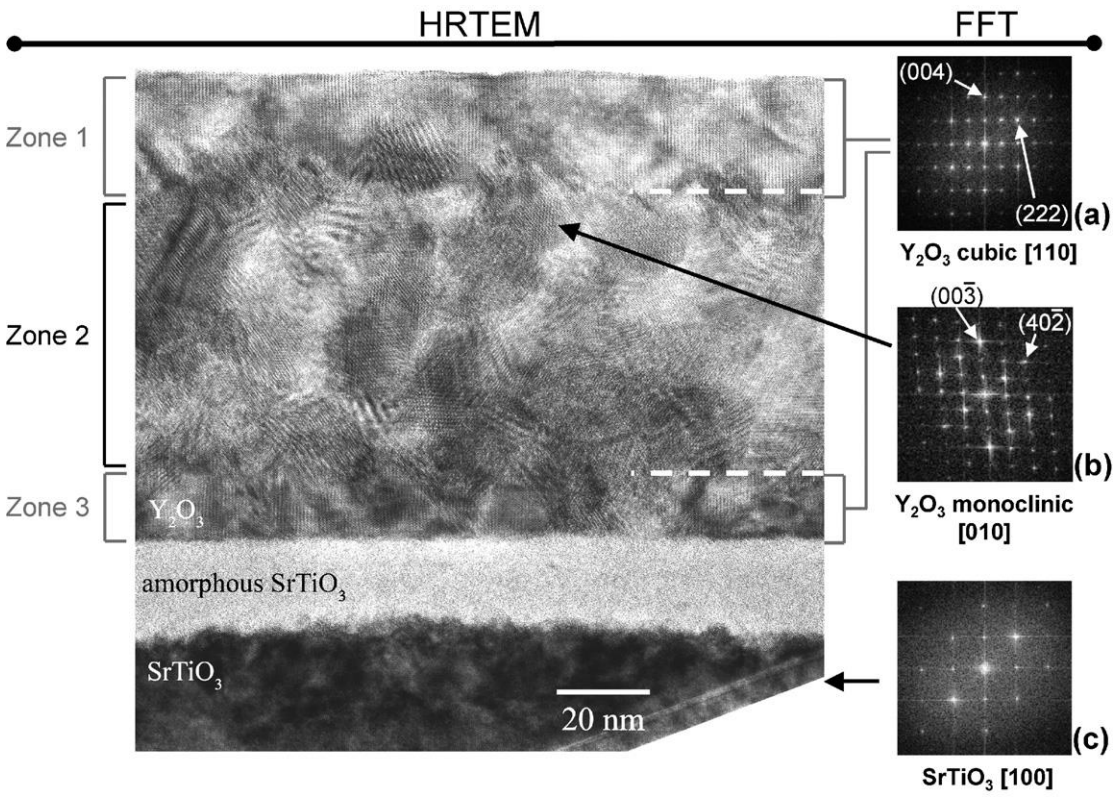

Fig. 6. HRTEM picture of a cross section sample of $Y_2O_3/SrTiO_3$ irradiated with 220 keV Xe^{2+} ions with a fluence of 3.6×10^{19} Xe^{2+}/m^2. (a-c) On the right side are the corresponding digital diffractograms.

The effects of very high energy implantation have also been studied. Y_2O_3 thin films deposited by IBS on the substrates Si, MgO and $SrTiO_3$ are implanted with 92 MeV Xe^{23+} at Ganil accelerator. These films have a thickness of 200 nm. The samples are exposed under normal incidence at a fluence of 4.6×10^{17} Xe^{2+}/m^2 with an ion flux of 8×10^{13} Xe^{2+}/m^2 s. The XRD and EELS characterisations of these film are in progress. The preliminary results show the vanishing of the Bragg peak corresponding to the in-plane reflection of the cubic structures (Ia3 and Fm3m) and the appearance of an another peak. This new peak location is neither characteristic of the fluorite nor the cubic-C structure. Furthermore, it does not correspond to the Bragg peak of a monoclinic structure as it has been shown in a previous work [13] on Y_2O_3 powders. The O K-edge profile not shown in this paper confirms this result. Irradiation performed with high energy on the Y_2O_3 thin film induces a different crystallographic phase transformation compared with what is obtained from medium energy irradiation. Even though the irradiation energy is very high, the thin yttrium oxide film is found to be still crystalline.

3. Conclusion

The Y_2O_3 thin films deposited by IBS are composed by a major fluorine crystallographic phase and a minor cubic-C phase. The main difference between these phases is the oxygen vacancy network. This cubic-C structure can be interpreted as a fluorite structure where one quarter of the anions is removed with a slight rearrangement of the remaining ones. Therefore the cubic-C exhibits an ordered network of the so-called structural oxygen vacancies. The cubic fluorite related (Fm3m) Bragg peak is due to a strong disorder of this oxygen network, which leads to strong disordering of the structural vacancy network. The consequence of this disorder is very important. First: according to previous investigation [6], it induces particular behaviours either on the dielectric properties or on the interfacial reactions between the oxide and the substrate particularly in the case of Y_2O_3 deposited on Si-SiO_x. Second: under medium energy implantation we observe a crystallo- graphic phase transition toward a monoclinic structure which is not observed if the film is composed of the cubic-C structure alone. Obviously, this fluorite-like phase of Y_2O_3 turns out to be of prime importance in the crystallographic phase change from the cubic to monoclinic induced by irradiation.

Acknowledgments

Serge Bouffard and Isabelle Monnet from CIRIL Laboratory in Caen are kindly acknowledged for providing the GANIL accelerator facilities.

References

[1] R.J. Gaboriaud, F. Pailloux, P. Guerin, F. Paumier, J. Phys., D, Appl. Phys. 33 (2000) 2884.
[2] F. Paumier, R.J. Gaboriaud, A. Kaul, Cryst. Eng. 5 (2002) 169.
[3] F.M. D'Heurle, J.M.E. Harper, Thin Solid Films 171 (1989) 81.
[4] H. Fukumoto, T. Imura, Y. Osaka, Appl. Phys. Lett. 55 (1989) 360.
[5] E.K. Evangelou, C. Wiemer, M. Fanciulli, M. Sethu, W. Cranton, J. Appl. Phys. 94 (1) (2003) 318.
[6] R.J. Gaboriaud, F. Pailloux, P. Guerin, F. Paumier, Thin Solid Films 400 (2001) 106.
[7] F. Paumier, R.J. Gaboriaud, Thin Solid Films 441 (2003) 307.
[8] R.J. Gaboriaud, F. Paumier, F. Pailloux, P. Guerin, Mater. Sci. Eng., B, Solid-State Mater. Adv. Technol. 109 (2004) 34.
[9] A.E. Solov'eva, Neorg. Mater. 21 (1985) 808.
[10] F. Pailloux, M. Jublot, R.J. Gaboriaud, M. Jaouen, F. Paumier, Phys. Rev., B 72 (2005) 125425.
[11] J.F. Ziegler, J.P. Biersack, U. Littmark, The Stopping and Range of Ions in Solids, Pergamon Press, New York, 1985.
[12] M. Tang, J.A. Valdez, P. Lu, G.E. Gosnell, C.J. Wetteland, K.E. Sickafus, J. Nucl. Mater. 328 (2004) 71.
[13] S. Hemon, C. Dufour, A. Berthelot, F. Gourbilleau, E. Paumier, S. Bégin-Collin, Nucl. Instrum. Methods Phys. Res., B Beam Interact. Mater. Atoms 166-167 (2000) 339.